

## Brightness Temperature of Radio Zebras and Wave Energy Densities in Their Sources

L.V. Yasnov<sup>1</sup> · J. Benáček<sup>2</sup> · M. Karlický<sup>3</sup>

Received ; accepted

© Springer ●●●

**Abstract** We estimated the brightness temperature of radio zebras (zebra pattern – ZP), considering that ZPs are generated in loops having an exponential density profile in their cross-section. We took into account that when in plasma there is a source emitting in all directions, then in the escape process from the plasma the emission obtains a directional character nearly perpendicular to the constant-density profile. Owing to the high directivity of the plasma emission (for emission at frequencies close to the plasma frequency) the region from which the emission escapes can be very small. We estimated the brightness temperature of three observed ZPs for two values of the density scale height (1 and 0.21 Mm) and two values of the loop width (1 and 2 arcsec). In all cases high brightness temperatures were obtained. For the higher value of the density scale height, the brightness temperature was estimated as  $1.1 \times 10^{15}$  –  $1.3 \times 10^{17}$  K, and for the lower value as  $4.7 \times 10^{13}$  –  $5.6 \times 10^{15}$  K. These temperatures show that the observation probability of a burst with ZP, which is generated in the transition region with a steep gradient of the plasma density, is significantly higher than for a burst generated in a region with smoother changes of the plasma density. We also computed the saturation energy density of the upper-hybrid waves (which according to the double plasma resonance model are generated in the zebra source) using a 3D particle-in-cell model with the loss-cone type of distribution of hot electrons. We found that this saturated energy is proportional to the ratio of hot electron and background plasma densities. Thus, comparing the growth rate and collisional damping of the upper-hybrid waves, we estimated minimal densities of hot electrons as well as the minimal value of the saturation energy density of the upper-hybrid waves. Finally, we compared the computed energy density of the upper-hybrid waves with the energy density of the electromagnetic waves in the zebra source and thus estimated the efficiency of the wave transformation.

---

<sup>1</sup> St.-Petersburg State University, St.-Petersburg, 198504, Russia (e-mail: l.yasnov@spbu.ru)

<sup>2</sup> Department of Theoretical Physics and Astrophysics, Masaryk University, Kotlářská 2, CZ – 611 37 Brno, Czech Republic (e-mail: jbenacek@physics.muni.cz)

<sup>3</sup> Astronomical Institute, Academy of Sciences of the Czech Republic, 251 65 Ondřejov, Czech Republic (e-mail: karlicky@asu.cas.cz)

---

**Keywords:** Sun: corona — Sun: flares — Sun: radio radiation

## 1. Introduction

Fine structures of solar radio bursts are very important for understanding flare energy-release processes and diagnostics of the flare plasma. Among various fine structures the most intriguing one is the zebra structure (ZP – zebra pattern) occurring in Type IV radio bursts. In radio spectra it appears as several parallel stripes distributed uniformly in frequency; see examples below. Usually the number of such zebra stripes in ZP is large ( $> 5 - 8$ , sometimes even exceeding 20).

There are still questions about the generation mechanism of these ZPs. Among many proposed models (Zheleznyakov and Zlotnik, 1975; LaBelle *et al.*, 2003; Bárta and Karlický, 2006; Kuznetsov and Tsap, 2007; Tan, 2010; Karlický, 2013), the most commonly accepted model is that based on the double-plasma resonance (DPR) (Zlotnik, 2013; Karlický and Yasnov, 2015). Based on this model, most of the observed characteristics of ZPs were explained: the frequency range, polarization, amount of stripes and their frequencies, their high-frequency limit, and their temporal changes.

However, up to now in the literature there are only a few estimations of the ZP brightness temperature, which is important for further specification of the generation mechanism of ZPs. For example, Chernov *et al.* (1994) estimated the brightness temperature of metric ZPs to be  $10^{10}$  K with the source size constrained by the Nançay Radioheliograph.

Further estimation of the ZP brightness temperature ( $T_b = 10^{13}$  K) was by Chernov, Yan, and Fu (2003), where the ZP consisted of spiky superfine structures; see also Chernov (2006). On the other hand, Chernov (2006) states that the metric ZP radio sources occupy a noticeable part of the background continuum source or even the entire active region. The half-width of one source of the metric ZP was about 1.9 arcmin, which gives a brightness temperature of  $10^{10}$  K.

Using the *Siberian Solar Radio Telescope* (SSRT), Altyntsev *et al.* (2005) observed a ZP burst at  $\approx 5.7$  GHz (the highest frequency ever reported for ZP emission), which yielded a lower limit of  $T_b \approx 2 \times 10^7$  K.

Chen *et al.* (2011) estimated the lower limit for the decimetric ZP brightness temperature as  $1.6 \times 10^9$  K. Finally, Tan *et al.* (2014) estimated the brightness temperature of a decimetric ZP as  $T_b \approx 2 \times 10^{11}$  K.

In the present article we estimate the brightness temperature of ZP considering that a ZP is generated in the loop having in its cross-section an exponential density profile. In this case, the ZP source size and brightness temperature depend on the loop cross-section size. Furthermore, using a 3D particle-in-cell model with the loss-cone type of distribution of hot electrons, we compute the energy density of the upper-hybrid waves. Then this energy density is compared with that of the electromagnetic waves and thus the efficiency of the wave transformation (which is not well known) is estimated.

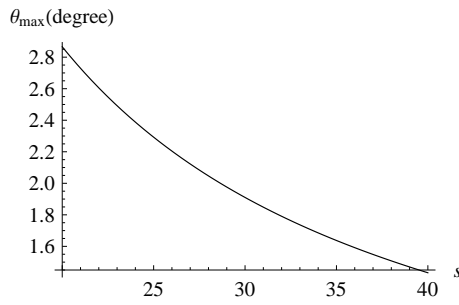


**Figure 1.** Maximum escape angle of the plasma emission in conditions of the double-plasma resonance depending on the gyro-harmonic number  $s$ .

## 2. Sizes of the Zebra Source

If in a plasma there is a source emitting in all directions then the emission during its escape process obtains directional character. The range of angles  $\leq \Theta_{\max}$ , in which the emission escapes, can be expressed as (Zheleznyakov, 1997)

$$\Theta_{\max} = \operatorname{arcsec} \left( \frac{\omega}{\omega_L} \right), \quad (1)$$

where  $\omega_L$  is the plasma frequency in the source and  $\omega$  is the emission frequency. In the conditions of a double-plasma resonance, the ratio of these frequencies is (Karlický and Yasnov, 2015)

$$\frac{\omega}{\omega_L} = \frac{s}{\sqrt{s^2 - 1}}, \quad (2)$$

where  $s$  is the gyro-harmonic number.

In Figure 1 the maximum escape angle of the plasma emission for the double-plasma resonance in the dependance on the gyro-harmonic number  $s$  is shown.

Owing to the high directivity of the plasma emission (for emission frequency close to the plasma frequency), the region from which the emission escapes can be very small. This is connected with the fact that the emission region in the flare loop at a fixed frequency is not flat, due to the density inhomogeneity across the loop (the maximum density is expected at the loop axis). It has a convex form and thus the emission with a high directivity (having the maximum value in the direction perpendicular to the constant-density layer) can reach an observer only from a limited region.

Watko and Klimchuk (2000) showed that the width of loops close to their foot-points, where the decimetric bursts are generated, is about 0.5 arcsec (0.36 Mm), and the typical width of higher loops is about 1 arcsec. Note that the decimetric ZPs are generated in loops at low heights (about 3 Mm) (Karlický and Yasnov, 2015; Yasnov, Karlický, and Stupishin, 2016). The width of some loops can be even smaller. For example, Peter *et al.* (2013) found tiny 1.5 MK loop-like structures that they interpret as miniature coronal loops. Their coronal segments above the chromosphere have a length of only about 1 Mm and a thickness

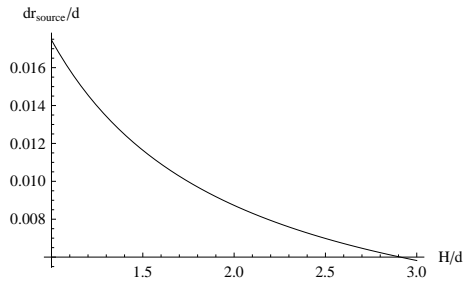


**Figure 2.** The source extent  $[\Delta r_{\text{source}}/d]$  as a function of  $H/d$  for the emission nearly perpendicular (for the maximum escape angle =  $2^\circ$ ) to the constant-density profile.

of less than 200 km. Moreover, Peter and Bingert (2012) showed that in a 3D self-consistent magnetohydrodynamic model of the solar corona, the loop width remains constant with height, and profiles of intensities along the loop radius correspond to gaussian ones. The gaussian profile along the loop radius was considered also by Chernov *et al.* (1994). Kuznetsov and Kontar (2015) assumed the gaussian function ( $\exp(-r^2/a^2)$ , where  $r$  is the loop radius and  $a = 1$  arcsec) describing the electron distribution in the flare loop.

Therefore, in agreement with the above-mentioned articles, we assume that the density inside the magnetic loop at a specific height  $[h_0]$  has the exponential form

$$n_e(r) = n_{\text{em}}(h_0) \exp\left(-\frac{r^2}{d^2}\right), \quad (3)$$

where  $n_{\text{em}}$  is the density at the loop axis,  $d$  is the loop width, and  $r$  is the radius across the loop. Moreover, the density in the loop decreases with the height as  $\approx \exp(-(h - h_0)/H)$ , where  $h$  is the height in the solar atmosphere and  $H$  is the scale height. Thus, the density inside the loop can be expressed as

$$n_e(r, h) = n_{\text{em}}(h_0) \exp\left(-\frac{r^2}{d^2}\right) \exp\left(-\frac{h - h_0}{H}\right). \quad (4)$$

Now, let us calculate the form of a layer with constant plasma density. For the height where this layer is located, we can write

$$C = n_{\text{em}}(h_0) \exp\left(-\frac{r^2}{d^2}\right) \exp\left(-\frac{h - h_0}{H}\right), \quad (5)$$

$$h(r) = h_0 - H \frac{r^2}{d^2} + H \ln\left(\frac{n_{\text{em}}(h_0)}{C}\right), \quad (6)$$

where  $C$  is a constant.

In a loop with constant magnetic field, from the pressure equilibrium and density variations it follows that the temperature varies, and thus also the scale-height. However, for simplification in further calculations, we assume that the scale-height  $[H]$  inside the loop is constant.

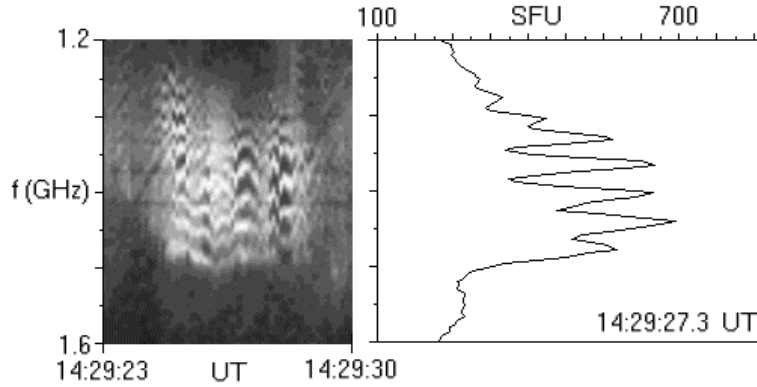


**Figure 3.** *Left panel:* An example of the zebra pattern observed by the Ondřejov radiospectrograph during the 2 May 1998 solar flare. *Right panel:* The radio-flux profile as a function of frequency at 14:29:27.3 UT.

Then the derivation of  $dh/dr$  is

$$\frac{dh}{dr} = -\frac{2Hr}{d^2}. \quad (7)$$

Using this derivation, the extent of the emission region for which the emission direction is nearly perpendicular to the constant-density profile can be estimated as

$$\Delta r_{\text{source}} = \frac{d^2 \tan(\Theta_{\text{max}})}{2H}, \quad (8)$$

where  $\Theta_{\text{max}}$  is the maximum escape angle of the plasma emission according to the Equation 1 (Figure 1). Note that the extent is independent of  $r$ . An example of the dependance of  $\Delta r_{\text{source}}/d$  on  $H/d$  for  $\Theta_{\text{max}} = 2^\circ$  degrees is shown in Figure 2.

The emission source is also extended in height. This dimension can be estimated as  $h_s = H(df/f)$ , where  $df$  is the bandwidth of the zebra stripe and  $f$  the zebra-stripe frequency.

### 3. Estimations of the Brightness Temperature of Zebra Structures

Now, let us estimate the brightness temperature of some observed ZPs. For this purpose we selected three ZPs observed by the Ondřejov radiospectrograph (Jiricka *et al.*, 1993); see Figures 3, 4, and 5.

The brightness temperature can be expressed as (Zaitsev and Stepanov, 1983)

$$T_b = \frac{S}{7 \times 10^{-11}} \frac{1}{f_{\text{GHz}}^2 L_8^2}, \quad (9)$$

where  $S$  is the radio flux in SFU,  $f_{\text{GHz}}$  is the frequency in GHz, and  $L_8$  ( $= 2\Delta r_{\text{source}}$ ) is the dimension of the emission region in units of  $10^8$  cm.

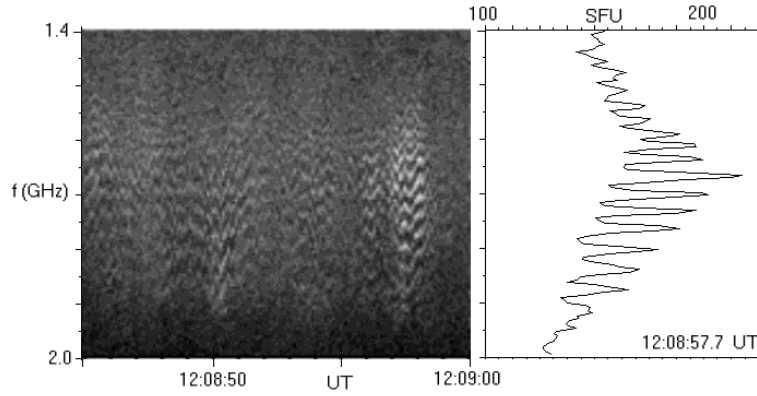


**Figure 4.** *Left panel:* An example of the zebra pattern observed by the Ondřejov radiospectrograph during the 14 February 1999 solar flare. *Right panel:* The radio-flux profile as a function of frequency at 12:08:57.7 UT.

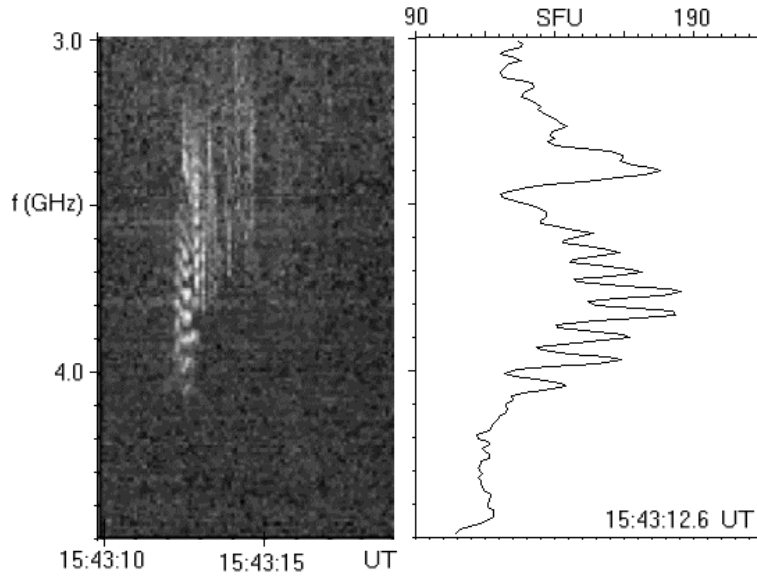


**Figure 5.** *Left panel:* An example of the zebra pattern observed by the Ondřejov radiospectrograph during the 6 June 2000 solar flare. *Right panel:* The radio-flux profile as a function of frequency at 15:43:12.6 UT.

Thus to compute the brightness temperature, we need to determine the source size  $[\Delta r_{\text{source}}]$ . First, using the method presented by Karlický and Yasnov (2015), we determined the gyro-harmonic numbers  $s_1$  for the observed zebra. Knowing  $s_1$  (see Table 1) and considering the scale height as  $H = 1$  Mm (according to the relation  $H$  [m] =  $50 T$  [K] (Priest, 2014) for the temperature  $T = 2 \times 10^4$  K), we calculated the source size of the observed zebra for two values of  $2d$  (1 and 2 arcsec). All of the computed parameters of the zebra sources together with the brightness temperatures are shown in Table 1.

**Table 1.** ZP source parameters.  $S$  is the radio flux in SFU units and  $s_1$  is the gyro-number of the stripe with the lowest frequency.

	ZP 2 May 1998	ZP 14 February 1999	ZP 6 June 2000
Event location	S15W15	N16E09	N23E15
$S$ [SFU]	650	170	210
$f_{\text{GHz}}$	1.45	1.67	3.78
$s_1$	21	32	34
$\Theta_{\text{max}}$	2.70	1.79	1.68
$L_8$ ( $2 d = 1$ arcsec)	0.0059	0.0038	0.0035
$L_8$ ( $2 d = 2$ arcsec)	0.023	0.015	0.014
$T_b$ ( $2 d = 1$ arcsec)	$13 \times 10^{16}$ K	$6 \times 10^{16}$ K	$1.7 \times 10^{16}$ K
$T_b$ ( $2 d = 2$ arcsec)	$0.83 \times 10^{16}$ K	$0.39 \times 10^{16}$ K	$0.11 \times 10^{16}$ K
Source height [km]	28	14.7	12.5

**Table 2.** ZP source parameters for  $H=0.21\text{Mm}$ .

	ZP 2 May 1998	ZP 14 February 1999	ZP 6 June 2000
$L_8$ ( $2 d = 1$ arcsec)	0.028	0.018	0.017
$L_8$ ( $2 d = 2$ arcsec)	0.11	0.070	0.067
$T_b$ ( $2 d = 1$ arcsec)	$5.6 \times 10^{15}$ K	$2.7 \times 10^{15}$ K	$0.73 \times 10^{15}$ K
$T_b$ ( $2 d = 2$ arcsec)	$0.36 \times 10^{15}$ K	$0.18 \times 10^{15}$ K	$0.047 \times 10^{15}$ K

However, in a region with a rapid change of the plasma temperature, the scale height can be shorter. Therefore, let us estimate the brightness temperature using the model by Selhorst, Silva-Válio, and Costa (2008). For typical densities in ZP sources  $5.0 \times 10^9 \text{ cm}^{-3} - 3.6 \times 10^{10} \text{ cm}^{-3}$  the model gives heights in the solar atmosphere between 2.84 Mm and 3.27 Mm. Thus, the scale height is  $H = 0.21$  Mm, which is almost five times shorter than that according to the formula of Priest used above. For such a scale height the ZP source parameters are given in Table 2.

#### 4. Energy Densities of Electromagnetic and Upper-Hybrid Waves in the ZP Source

Let us consider the zebra observed during the 2 May 1998 event. Knowing the ZP radio flux (650 SFU) and the zebra line frequency width (40 MHz), and computing the ratio of the emission area at 1 AU (corresponding to the emission directivity angle ( $2.7^\circ$  for  $s = 21$ , see Figure 1)), and ZP source area ( $L_8 \times L_8$  for four cases according to Tables 1 and 2), the energy density of electromagnetic waves in the ZP source is calculated; see the second column in Table 3.

In the double plasma resonance (DPR) model of ZPs, it is assumed that in the ZP source there are hot electrons with a loss-cone type distribution together with much denser background plasma. The distribution is unstable and generates the upper-hybrid waves that after their transformation produce the observed ZPs.

Therefore, besides the estimation of the energy density of electromagnetic waves, it is highly desirable to estimate the energy density of the upper-hybrid waves in the ZP source. For this purpose we use a 3D particle-in-cell (PIC) relativistic code (Buneman and Storey, 1985, Matsumoto and Omura, 1993, Karlický and Bárta, 2008). Although this code is very useful for such computations, it has its own limitations. Therefore some parameters of the ZP of 2 May 1998 cannot be reproduced in the following PIC computations. For example, there is a problem in making computations with high gyro-harmonic numbers ( $s > 20$  in our case) because it is very difficult to select PIC plasma parameters reproducing resonances with high-harmonic numbers, especially due to the discrete space (grids) in PIC models.

The size of the model is  $L_x \times L_y \times L_z = \lambda \Delta \times \lambda \Delta \times 32 \Delta$ , where  $\Delta$  is the grid size and  $\lambda$  is the wavelength of the upper-hybrid wave in resonance in normalized units. We chose a model containing only one wavelength of the upper-hybrid wave to simplify the processing and decrease computing time. The model time step is  $dt = 1$ , plasma electron frequency  $\omega_{pe} dt = 0.05$ , initial magnetic field is in  $z$ -direction, electron-cyclotron frequency is, e.g.,  $\omega_{ce} = 0.176 \omega_{pe}$  for the harmonic number  $s = 7$ . The harmonic number is considered in the interval  $s = 4 - 18$ . We use two groups of electrons: a) cold background electrons with the thermal velocity  $v_{tb} = 0.03 c$  ( $c$  is the light speed), corresponding to temperature 5.35 MK, and b) hot electrons with the DGH (Dory, Guest, and Harris, 1965) distribution function for  $j = 1$  in the form

$$f = \frac{u_{\perp}^2}{2(2\pi)^{3/2}v_t^5} \exp\left(-\frac{u_{\perp}^2 + u_{\parallel}^2}{2v_t^2}\right), \quad (10)$$

where  $u_{\perp} = p_{\perp}/m_e$  and  $u_{\parallel} = p_{\parallel}/m_e$  are electron velocities and  $p_{\perp}$  and  $p_{\parallel}$  are components of the electron momentum perpendicular and parallel to the magnetic field,  $m_e$  is the electron mass, and  $v_t = 0.2 c$  is the thermal spread in the velocities of hot electrons.

The electron density of cold electrons per cell was taken as  $n_e = 1920$  and the ratio of hot and background plasma electrons as  $n_h/n_e = 1/8$ . We also made computations with  $n_h/n_e = 1/16$  and  $1/32$  to know the dependence of the saturation energy of the upper-hybrid waves on the density ratio  $n_h/n_e$ . The number of protons is the same as electrons and their temperature is the same as that of cold electrons.

Using this PIC code, the temporal evolution of the energy of the upper-hybrid waves  $[W_{UH}]$ , generated by hot electrons, for  $s = 7$  and three values of  $n_h/n_e$  are shown in Figure 6 left. As can be seen here, the ratio of the saturated energy of the upper-hybrid waves to the kinetic energy of hot electrons is in all three cases the same ( $W_{UH} = 8 \times 10^{-3} E_{h,kin}$ ). This means that the saturated energy of the upper-hybrid waves is proportional to the  $n_h/n_e$  ratio because  $E_{h,kin}$  depends on  $n_h$ . The saturated energy of the upper-hybrid waves also depends

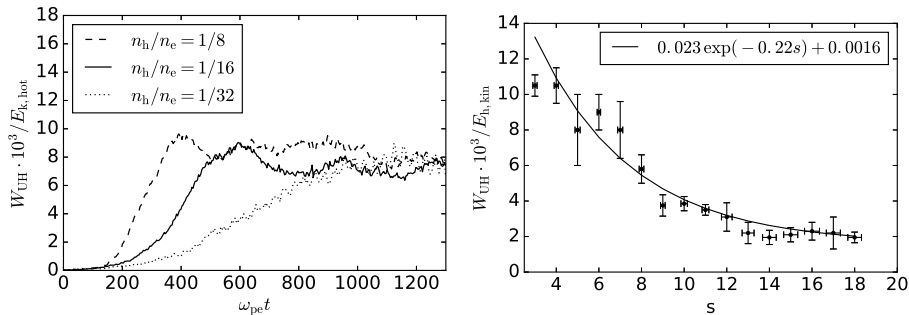


**Figure 6.** *Left:* Temporal evolution of the ratio of the energy of the upper-hybrid waves  $W_{\text{UH}}$  to the kinetic energy of hot electrons  $E_{\text{h,kin}}$  for  $s = 7$  and three values of  $n_{\text{h}}/n_{\text{e}}$ . *Right:* The ratio of the saturated energy of the upper-hybrid waves to the kinetic energy of hot electrons for  $n_{\text{h}}/n_{\text{e}} = 1/8$  as a function of  $s$ . The full line shows the exponential fit.

**Table 3.** Energy densities of electromagnetic and upper-hybrid waves in the ZP source for the 2 May 1998 event.  $\epsilon = W_{\text{elm}}/W_{\text{UH,min}}$  is the parameter expressing the efficiency of transformation of the upper-hybrid waves into electromagnetic ones.

$L_8$ [Mm]	$W_{\text{elm}}$ [J m <sup>-3</sup> ]	$W_{\text{UH,min}}$ [J m <sup>-3</sup> ]	$\epsilon$
0.0059	$3.90 \times 10^{-8}$	$4.40 \times 10^{-5}$	$8.86 \times 10^{-4}$
0.023	$2.57 \times 10^{-9}$	$4.40 \times 10^{-5}$	$5.84 \times 10^{-5}$
0.028	$1.73 \times 10^{-9}$	$4.40 \times 10^{-5}$	$3.93 \times 10^{-5}$
0.11	$1.12 \times 10^{-10}$	$4.40 \times 10^{-5}$	$2.54 \times 10^{-6}$

on  $s$  as shown in Figure 6 right. The computed values can be well fitted by the exponential fit. Therefore, for the 2 May 1998 zebra that was analyzed, where  $s = 21$ , we use this exponential fit, which gives the value of the saturated energy of the upper-hybrid waves as  $W_{\text{UH}} = 1.6 \times 10^{-3} E_{\text{h,kin}}$ , where  $E_{\text{h,kin}}$  is the kinetic energy of hot electrons.

Now, for the following estimations, let us derive the minimum value of the parameter  $n_{\text{h}}/n_{\text{e}}$ . For this purpose we used the analytical expression for the growth rate of the upper-hybrid waves as derived by Thejappa (1991)

$$-\gamma_{\text{UH}} \approx 4.4 \times 10^{-2} \omega_{\text{pe}} \frac{n_{\text{h}}}{n_{\text{e}}}. \quad (11)$$

This growth rate agrees with that in our PIC simulations. To generate the upper-hybrid waves this growth rate needs to be greater than the damping of these waves by collisions,

$$\gamma_{\text{c}} = 2.75 \frac{n_{\text{e}}}{T_{\text{e}}^{3/2}} \ln \left( 10^4 T_{\text{e}}^{3/2} / n_{\text{e}}^{1/3} \right), \quad (12)$$

where  $T_e$  is the background plasma temperature. Thus, when we put  $\gamma_{UH}$  equal to  $\gamma_c$ , then for the mean ZP frequency (1.45 GHz and corresponding plasma density  $n_e = 2.6 \times 10^{16} \text{ m}^{-3}$ ) and for  $T_e$  in the ZP source as  $2 \times 10^4 \text{ K}$  (at bottom of the transition region), the minimal ratio of  $n_h/n_e$  is  $4.93 \times 10^{-4}$ .

Now, if we take the density of the hot electrons in the ZP source as equal to the minimum density  $n_h = 2.6 \times 10^{16} \times 4.93 \times 10^{-4} = 1.28 \times 10^{13} \text{ m}^{-3}$  and utilizing the extrapolated value of the saturated energy of the upper-hybrid waves for  $s = 21$  and the linear dependance of the saturated energy of the upper-hybrid waves on  $n_h$ , found in the PIC simulations, then the minimum energy density of the upper-hybrid waves  $W_{UH,\min}$  is calculated; see the third column in Table 3.

Then, if we assume that the energy density of the upper-hybrid waves in the ZP source from 2 May 1998 is the same as  $W_{UH,\min}$ , then we can calculate the parameter expressing the efficiency of transformation of the upper-hybrid waves into electromagnetic ones; see the last column in Table 3. However, the ratio  $n_h/n_e$  in real conditions needs to be greater than its minimum value, and therefore  $\epsilon$  in real conditions should be lower. On the other hand, values of the parameter  $\epsilon$  would be greater if we considered the absorption of the electromagnetic waves near the ZP source.

## 5. Discussion and Conclusions

The closeness of the emission frequency of decimetric zebras to the plasma frequency determines a narrow directivity of the ZP emission. For the exponential density profile across the flaring loop, it gives a small area of such emission and thus high brightness temperatures. We considered two variants of the density dependance on height, *i.e.*, two values of the scale height: 1 Mm according to the formula of Priest (2014) and 0.21 Mm for the transition region (Selhorst, Silva-Válio, and Costa, 2008), and two values for the loop width (1 and 2 arcseconds). In all cases high brightness temperatures were obtained. For the higher value of the density scale height the brightness temperature was estimated as  $1.1 \times 10^{15} - 1.3 \times 10^{17} \text{ K}$ , and for the lower value it was estimated as  $4.7 \times 10^{13} - 5.6 \times 10^{15}$ .

As shown in the Introduction, previous estimations of the ZP brightness temperature were noticeably lower (from  $2 \times 10^7$  to  $10^{13} \text{ K}$ ). The high brightness temperature found here together with short duration of zebras and their frequent strong polarization can only be explained as generated by the coherent emission mechanism. Namely, in the non-coherent emission mechanism, the brightness temperature cannot be higher than  $10^{12} \text{ K}$ , which is given by the Compton limit. The mechanism of the coherent emission of the plasma waves (including the upper-hybrid waves considered here) is described in detail, *e.g.* by Fleishman and Mel'nikov (1998). Here, we only mention that for the processes described in the present article an anisotropic distribution of superthermal electrons is necessary. As shown by Yasnov and Karlický (2015) the most probable location of the zebra generation is the transition region in the solar atmosphere of active regions. In the transition region the temperature as well as the pressure changes rapidly, and thus the magnetic fields fan out to form funnels; see,

e.g. Wiegmann, Thalmann, and Solanki (2014). In such magnetic field funnels superthermal electrons with momentum perpendicular to the magnetic field are more numerous than those with parallel momentum. The consequence is that in this spatially small region the high level of anisotropy of the superthermal electrons is easily reached, and thus the upper-hybrid waves are generated there (Benáček, Karlický, and Yasnov, 2017).

Note that these brightness temperatures are close to the brightness temperatures of decimetric spikes (Benz, 1986), which indicates that energies of electrons in the two types of bursts are similar. Because the emission frequency is close to the plasma frequency, the emission absorption can be high and thus the brightness temperature can be even higher.

Observed sizes of ZP sources can be larger than those assumed here because they are enlarged by the scattering of the emission on density fluctuations in the corona (Bastian, 1994).

We found a lower brightness temperature for a shorter scale height. It is indicated independently in findings presented by Yasnov and Karlický (2015), Karlický and Yasnov (2015) and Yasnov, Karlický, and Stupishin (2016) that the observational probability of a burst with zebras, which is generated in the transition region with a steep density gradient, is generally greater than the burst generated in the region with smoother changes of the plasma density. This is caused by an enlargement of the visible emission area in the atmosphere with the high density gradient.

Note that sometimes ZPs appear on the radio spectrum of a Type IV (continuum) burst irregularly or quasi-periodically (on timescales of seconds). It can be explained by small irregular or quasi-periodic motions of the flare loop in the case when the ZP source area is sufficiently small. Then the narrow cone of the emission directivity is oriented toward an observer and the zebra is observed, or vice versa.

Numerical simulations with the 3D particle-in-cell model having hot electrons described by the DGH distribution function show that firstly the energy density of the upper-hybrid waves exponentially grows with the linear growth rate and then it is saturated. We found that the saturation energy of the upper-hybrid waves is proportional to the ratio  $n_h/n_e$ . This dependance enabled us to calculate the saturation energy of the upper-hybrid waves for much smaller ratios of  $n_h/n_e$ . The saturation energy of the upper-hybrid waves also depends on the gyroharmonic number  $s$ . For  $s = 7 - 18$  we found that the computed saturated energies can be well fitted by a exponential function. This fit enables us to find the saturated energy of the upper-hybrid waves for the analyzed 2 May 1998 zebra with  $s = 21$  as about  $W_{UH} = 1.6 \times 10^{-3} E_{h,kin}$ .

The upper-hybrid waves are generated when the growth rate exceeds the damping of these waves by collisions. For the zebra observed during the 2 May 1998 event this condition is fulfilled if the ratio of hot and cold electrons  $n_h/n_e$  is greater than  $4.93 \times 10^{-4}$ . Using this value we computed the minimum energy density of the upper-hybrid waves in ZP source ( $W_{UH,min} = 4.40 \times 10^{-5} \text{ J m}^{-3}$ ) and the transformation efficiency of the upper-hybrid waves into electromagnetic ones ( $\epsilon = 2.54 \times 10^{-6} - 8.86 \times 10^{-4}$ ).

The transformation efficiency strongly depends on plasma parameters in the radio source such as plasma turbulence, levels of low-frequency plasma waves (*e.g.* the ion-sound waves), and density gradients (Melrose, 1985). Unfortunately, most of these parameters in ZP sources are not known, and moreover the theory of wave conversions is not fully established, especially in the non-linear regime. For example, Melrose (1985) presents this efficiency in the very broad range from  $10^{-10}$  for the scattering on the thermal ions to  $10^{-4}$  for the small-scale density inhomogeneities ( $10 - 10^2$  km). Comparing now the transformation efficiency found in the present article with those shown by Melrose (1985), we think that in the zebra source there are small-scale density inhomogeneities.

**Acknowledgements** The authors thank the referee for constructive comments that improved the article. M. Karlický acknowledges support from Grants 16-13277S and 17-16447S of the Grant Agency of the Czech Republic. L.V. Yasnov acknowledge support from Grant 16-02-00254 of the Russian Foundation for Basic Research. Computational resources were provided by the CESNET LM2015042 and the CERIT Scientific Cloud LM2015085, provided under the programme “Projects of Large Research, Development, and Innovations Infrastructures“

## Disclosure of Potential Conflicts of Interest

Authors have no potential conflict of interest.

## References

- Altyntsev, A.T., Kuznetsov, A.A., Meshalkina, N.S., Rudenko, G.V., Yan, Y.: 2005, On the origin of microwave zebra pattern. *Astron. Astrophys.* **431**, 1037. DOI. ADS.
- Bárta, M., Karlický, M.: 2006, Interference patterns in solar radio spectra: High-resolution structural analysis of the corona. *Astron. Astrophys.* **450**, 359. DOI. ADS.
- Bastian, T.S.: 1994, Angular scattering of solar radio emission by coronal turbulence. *Astrophys. J.* **426**, 774. DOI. ADS.
- Benáček, J., Karlický, M., Yasnov, L.: 2017, Temperature dependent growth rates of the upper-hybrid waves and solar radio zebra patternss. *Astron. Astrophys.* **555**, A1. DOI. ADS.
- Benz, A.O.: 1986, Millisecond radio spikes. *Solar Phys.* **104**, 99. DOI. ADS.
- Buneman, O., Storey, L.R.O.: 1985, Simulations of fusion plasmas by A 3-D, E-M particle code. Technical report, Stanford Univ. Report, Stanford. ADS.
- Chen, B., Bastian, T.S., Gary, D.E., Jing, J.: 2011, Spatially and spectrally resolved observations of a zebra Pattern in a solar decimetric radio burst. *Astrophys. J.* **736**, 64. DOI. ADS.
- Chernov, G.P.: 2006, Solar Radio Bursts with Drifting Stripes in Emission and Absorption. *Space Sci. Rev.* **127**, 195. DOI. ADS.
- Chernov, G.P., Yan, Y.H., Fu, Q.J.: 2003, A superfine structure in solar microwave bursts. *Astron. Astrophys.* **406**, 1071. DOI. ADS.
- Chernov, G.P., Klein, K.-L., Zlobec, P., Aurass, H.: 1994, Fine structure in a metric type 4 burst: Multi-site spectrographic, polarimetric, and heliographic observations. *Solar Phys.* **155**, 373. DOI. ADS.
- Dory, R.A., Guest, G.E., Harris, E.G.: 1965, Unstable Electrostatic Plasma Waves Propagating Perpendicular to a Magnetic Field. *Physical Review Letters* **14**, 131. DOI. ADS.
- Fleishman, G.D., Mel'nikov, V.F.: 1998, Reviews of Topical Problems: Millisecond solar radio spikes. *PHYSICS USPEKHI* **41**, 1157. DOI. ADS.
- Jiricka, K., Karlicky, M., Kepka, O., Tlamicha, A.: 1993, Fast drift burst observations with the new Ondrejov radiospectrograph. *Solar Phys.* **147**, 203. DOI. ADS.

- Karlický, M.: 2013, Radio continua modulated by waves: Zebra patterns in solar and pulsar radio spectra? *Astron. Astrophys.* **552**, A90. DOI. ADS.
- Karlický, M., Bárta, M.: 2008, Fragmentation of the Current Sheet, Anomalous Resistivity, and Acceleration of Particles. *Solar Phys.* **247**, 335. DOI. ADS.
- Karlický, M., Yasnov, L.V.: 2015, Determination of plasma parameters in solar zebra radio sources. *Astron. Astrophys.* **581**, A115. DOI. ADS.
- Kuznetsov, A.A., Kontar, E.P.: 2015, Spatially Resolved Energetic Electron Properties for the 21 May 2004 Flare from Radio Observations and 3D Simulations. *Solar Phys.* **290**, 79. DOI. ADS.
- Kuznetsov, A.A., Tsap, Y.T.: 2007, Loss-cone instability and formation of zebra patterns in type IV solar radio bursts. *Solar Phys.* **241**, 127. DOI. ADS.
- LaBelle, J., Treumann, R.A., Yoon, P.H., Karlický, M.: 2003, A model of zebra emission in solar type IV radio bursts. *Astrophys. J.* **593**, 1195. DOI. ADS.
- Matsumoto, H., Omura, Y.: 1993, *Computer space plasma physics: simulation techniques and software*, Terra Scientific, Tokyo, 305.
- Melrose, D.B.: 1985, In: McLean, D.J., Labrum, N.R. (eds.) *Plasma emission mechanisms*, Cambridge University Press, Cambridge, 177. ADS.
- Peter, H., Bingert, S.: 2012, Constant cross section of loops in the solar corona. *Astron. Astrophys.* **548**, A1. DOI. ADS.
- Peter, H., Bingert, S., Klimchuk, J.A., de Forest, C., Cirtain, J.W., Golub, L., Winebarger, A.R., Kobayashi, K., Korreck, K.E.: 2013, Structure of solar coronal loops: from miniature to large-scale. *Astron. Astrophys.* **556**, A104. DOI. ADS.
- Priest, E.: 2014, *Magnetohydrodynamics of the Sun*, Cambridge University Press, UK. ADS.
- Selhorst, C.L., Silva-Válio, A., Costa, J.E.R.: 2008, Solar atmospheric model over a highly polarized 17 GHz active region. *Astron. Astrophys.* **488**, 1079. DOI. ADS.
- Tan, B.: 2010, A physical explanation of solar microwave zebra pattern with the current-carrying plasma loop model. *Astrophys. Space Sci.* **325**, 251. DOI. ADS.
- Tan, B., Tan, C., Zhang, Y., Huang, J., Mészárosóvá, H., Karlický, M., Yan, Y.: 2014, A very small and super strong zebra pattern burst at the beginning of a solar flare. *Astrophys. J.* **790**, 151. DOI. ADS.
- Thejappa, G.: 1991, A self-consistent model for the storm radio emission from the sun. *Solar Phys.* **132**, 173. DOI. ADS.
- Watko, J.A., Klimchuk, J.A.: 2000, Width Variations along Coronal Loops Observed by TRACE. *Solar Phys.* **193**, 77. DOI. ADS.
- Wiegmann, T., Thalmann, J.K., Solanki, S.K.: 2014, The magnetic field in the solar atmosphere. *Astron. Astrophys. Rev.* **22**, 78. DOI. ADS.
- Yasnov, L.V., Karlický, M.: 2015, Regions of Generation and Optical Thicknesses of dm-Zebra Lines. *Solar Phys.* **290**, 2001. DOI. ADS.
- Yasnov, L.V., Karlický, M., Stupishin, A.G.: 2016, Physical Conditions in the Source Region of a Zebra Structure. *Solar Phys.* **291**, 2037. DOI. ADS.
- Zaitsev, V.V., Stepanov, A.V.: 1983, The plasma radiation of flare kernels. *Solar Phys.* **88**, 297. DOI. ADS.
- Zheleznyakov, V.V.: 1997, *Radiation in astrophysical plasmas [in Russian]; Original Russian Title — “Izlučeniye v astrofizicheskoy plazme”*, Yanus-K, Moscow. ADS.
- Zheleznyakov, V.V., Zlotnik, E.Y.: 1975, Cyclotron wave instability in the corona and origin of solar radio emission with fine structure. III. Origin of zebra-pattern. *Solar Phys.* **44**, 461. DOI. ADS.
- Zlotnik, E.Y.: 2013, Instability of electrons trapped by the coronal magnetic field and its evidence in the fine structure (zebra pattern) of solar radio spectra. *Solar Phys.* **284**, 579. DOI. ADS.